

Effect of taper tension profile on the telescoping in a winding process of high speed roll to roll printing systems[†]

Changwoo Lee¹, Hyunkyoo Kang², Hojoon Kim² and Keehyun Shin^{2,*}

¹*Flexible Display Roll to Roll Research Center, Konkuk University, 1 Hwayang-Dong, Gwangjin-Gu, Seoul 143-701, Korea*

²*Department of Mechanical and Aerospace Engineering, Konkuk University, 1 Hwayang-Dong, Gwangjin-Gu, Seoul 143-701, Korea*

(Manuscript received February 13, 2009; Revised July 14, 2009; Accepted August 6, 2009)

Abstract

Winding is an integral operation in almost every roll to roll system. A center-wound roll is one of the suitable and general schemes in a winding mechanism. In general, the quality of wound roll is known to be related to the lateral displacement error and starring defect of a wound roll. Especially, a telescoping within a center-wound roll can cause damages such as misalignment between layers, folding, wrinkle, etc. Taper tension is known to be one of the major factors which affect the shape of a wound roll. It is therefore necessary to analyze the relationship between taper tension profile and telescoping within the center-wound roll to prevent winding failure and to sustain high quality of the printed materials. It is hard to compensate for undesirable winding roll shapes such as telescoping, because a winding is commonly a final process in roll to roll systems and has no feedback control mechanism to correct winding roll shape directly during winding operation. Therefore, an optimal taper tension profile and the accurate control of it in a winding section could be one way to shape the fail-safe of a wound roll. Through the correlation between taper tension profile and telescoping in a winding process, a mathematical model for the telescoping due to tension distribution in cross machine direction was developed, and verified by experimental study. A new logic to determine the proper taper tension profile was designed by combining and analyzing the winding mechanism which includes nip induced tension model, relationship between taper tension profile and telescoping, relationship between taper value and telescoping. Numerical simulations and experimental results show that the proposed method is very useful for determining the desirable taper tension profile during the winding process and preventing defects of winding roll shape such as telescoping.

Keywords: Lateral displacement; Roll to roll system; Taper tension profile; Telescoping; Winding process; Wound roll

1. Introduction

Winding, which is a useful storage method without folding or cutting, is an integral operation and the final process in most roll to roll systems. A winding is the process of turning a flat web into a coil as shown in Fig. 1 [1, 2].

There are three kinds of winding mechanism as

shown in Fig. 2. The simplest is the center-wind where the roll is completely supported and driven through its core. The drive, which is usually a speed controlled electric motor, pulls web tension. The center-wind only has tension to control the hardness of a wound roll, and is one of the most efficient and convenient processes for a high speed winding process. Another common class of winding is the surface wind. In this winding method, the winding roll is nipped against a roll that is driven. The nip load is usually adjusted by a pneumatic or hydraulic cylinder system. The drive operates on the surface of the winding roll.

[†] This paper was recommended for publication in revised form by Associate Editor Kyung-Soo Kim

*Corresponding author. Tel.: +82 2 450 3072, Fax.: +82 2 447 5886

E-mail address: khshin@konkuk.ac.kr

© KSME & Springer 2009

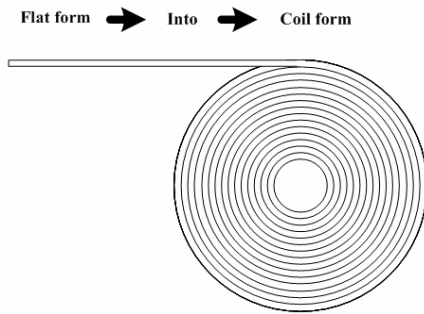


Fig. 1. Winding process.

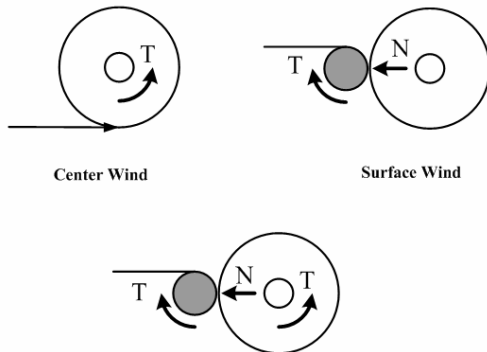


Fig. 2. Classifications of winder.

The wound roll hardness for surface winder is controlled by both web tension and nip load. The surface winding method is generally applied to the winding of very light substrate because excessive radial stress could be generated around core which makes defects such as buckling, starring, etc. The last class, the center-surface winder, can control roll hardness by adjusting web tension, as do both center and surface winders. The center-surface winder can also control winding hardness by varying the nip force, as does the surface winder. However, there are some difficulties in center-surface winding scheme such as synchronization of two independent driving motors (surface and center winder), high precision control of speed, friction between surface roll and winder [3-6].

Winding has a tension profile to control the hardness of wound roll in general. The tension is defined as the average machine direction web force per unit of web width. The web may neck, yield or break frequently when the tension is too high. If the tension is too low, the web may flop around or lose traction on rollers. In the same way, high radial stresses make the wound roll tight and low radial stresses make the wound roll loose [4-7]. The shape of wound roll can

be collapsed in both cases. There are three principles in roll structuring [6]. The first is that the roll must be wound harder at the beginning of winding in order to build a solid foundation. If the roll is too soft to be loose at the core, it may telescope upon unwinding. The second principle is that the web has to be wound softly at the end of winding. If the finish is overly hard or tight, then material might be damaged (starring, buckling, etc). Finally, the tightness varies smoothly from the tighter core to the looser finish as the roll builds. If there are abrupt changes in nip force or tension, then the roll may be prone to starring. In general, the hardness of wound roll is a function of tension, nip force and torque. It is, however, not easy to change the nip force in real-time, because a nipping system adjusted by a pneumatic or hydraulic cylinder has a low response time in general. On the other hand, the tension can be easily adjusted by controlling the speed of winding. That is, taper tension usually implies a reduction of web tension as a function of current roll diameter. The most common option of roll structuring is a linear taper tension with respect to current roll diameter. The most common scheme of winder control uses a starting point tension at the core and a slope to decrease winding tension as the roll diameter builds. This slope is usually entered as a percentage called *taper* [5, 6].

Altmann provided a general solution of a linear elastic roll material while using a nonlinear constitutive relation to find the radial and hoop stresses for successive wraps [8]. He solved a second-order differential equation for linear elastic material in a center wound roll. Altmann had considerable insight into the nondimensionalization of the elastic and geometric parameters so that the derivation did not become unwieldy. Yagoda established the core compliance as an inner boundary condition on center wound rolls [9]. He developed a hypergeometric series evaluation of the winding integral to correct Altmann's solution near the core and developed his model with the same integral formulation as Altmann. Hakiel incorporated nonlinear material properties into the basic mechanics and derived numerical solutions of wound roll stresses [7]. He was the first to publish a nonlinear solution using finite difference techniques. While previous and simpler winding models were able to reduce much of the solution to closed form expressions, the complexities of a nonlinear modulus precluded a predominantly mathematical treatment. Instead, the Hakiel model relies heavily on numerical

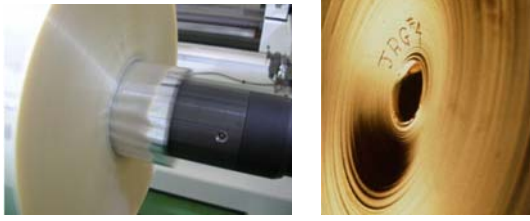


Fig. 3. Telescoping defect in a wound roll.

approximations of the winding differential equation. This numerical approach freed the evolution of winding models from more restrictive descriptions. Good et al. compared results of Hakiel’s model with inter-layer pressure measured by using pull tabs [2]. They noted that the predicted stresses were twice as large as the measured values. However, they were able to bring predicted and measured values into better agreement by modifying the outer hoop-stress boundary condition to relax relative to the out-layer tensile stresses by their model of “wound on tension” loss. Burns [1] derived a strain-based formula for stresses in profiled center wound rolls by using a residual stress model. In general, the residual stress depends on roll radius through the web tension as the outer layer is placed on to the roll. Thus this stress depends on the roll radius ratio and on how the roll is profiled.

Finally, it is clear from reviewing the literature that a momentous factor for making high quality wound roll is the taper tension profile in the winding process. Previous studies on the taper tension profile were focused on optimal radial stress distribution to minimize starring, buckling, etc. However, they did not relate their analysis to the lateral position error (telescoping) as shown in Fig. 3. Therefore, what is needed is to: (1) analyze the correlation between taper tension profile and telescoping, which is the result of the lateral instability of a moving web by tension variation, (2) analyze the relationship between slippage and operating conditions, (3) develop a mathematical model of the telescoping in a winding process, and (4) experimentally verify the performance of the proposed model.

2. Mathematical models

2.1 Taper tension profiles

Fig. 4 shows the schematic geometry of the tension T acting on the web and wound roll: a is core radius, R is current radius of the wound roll, M is torque, and σ_w is a taper tension profile.

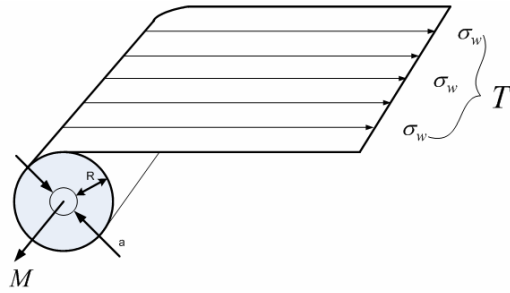


Fig. 4. Schematic of a center wound roll.

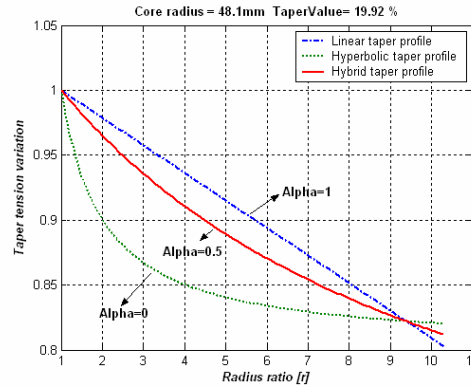


Fig. 5. Taper tension profiles in a winding process.

In general, linear and hyperbolic taper tension profiles were applied to a winding process [2, 7]. Those can be represented as the following Eqs. (1) and (2) respectively. Additionally, a hybrid taper tension profile could be used [3, 4]. It is designed by combining advantages of both linear and hyperbolic taper tension profiles. Eq. (3) shows the mathematical model of hybrid taper tension profile. σ_0 is initial web stress, $taper$ is the decrement of a winding tension, r is a dimensionless roll radius ratio, i.e., the wound roll radius R divide by the core radius a . In Eq. (3), α is the hybrid factor which is used for changing a shape of taper tension profile. That is, linear and hyperbolic taper profiles could be generated by using a hybrid taper tension model as shown in Fig. 5.

$$\sigma_{linear}(r) = \sigma_0 \left[1 - \left(\frac{taper}{100} \right) \frac{(r-1)}{(R-1)} \right] \tag{1}$$

$$\sigma_{hyperbolic}(r) = \sigma_0 \left[1 - \left(\frac{taper}{100} \right) \left(\frac{r-1}{r} \right) \right] \tag{2}$$

$$\sigma_{hybrid}(r) = \sigma_0 \left[1 - \left(\frac{taper}{100} \right) \frac{(r-1)}{(r + \alpha \cdot (R-r-1))} \right] \tag{3}$$

2.2 Taper tension profiles considering nip induced tension

Most of the winding is accomplished via a center winding technique in which a wound roll is directly driven by a motor and a lay-on roller is nipped on surface as shown in Fig. 6. The main purpose of the undriven nip roller (lay-on roller) is to help exude wound-in air from the wound roll.

Compressive force by the lay-on roll generates an additional web tension, the nip-induced tension [9]. A resultant taper tension including the nip induced tension can be presented as Eq. (4) with additional term of NIT.

$$\sigma_{w_total} = \sigma_w + NIT = \sigma_w + \frac{\mu N}{h} \tag{4}$$

where N is the nip load which may vary with respect to build up ratio, μ is the coefficient of friction between each layer of the web, and h is the web thickness.

The linear taper tension model including nipping effect (Eq. (5)) can be derived from Eq. (1) and Eq. (4). Substitution of Eq. (2) into Eq. (4) yields the hyperbolic taper tension model including the nipping force as shown in Eq. (6). Eq. (7) is the hybrid taper tension model with nip induced tension. In general, the nip load N for preventing air entrainment is set to become lower as the radius of the wound roll increases.

$$\sigma_w(r) = \sigma_0 \left[1 - \left(\frac{taper}{100} \right) \frac{(r-1)}{(R-1)} \right] + \frac{\mu N(r)}{h} \tag{5}$$

$$\sigma_w(r) = \sigma_0 \left[1 - \left(\frac{taper}{100} \right) \left(1 - \frac{1}{r} \right) \right] + \frac{\mu N(r)}{h} \tag{6}$$

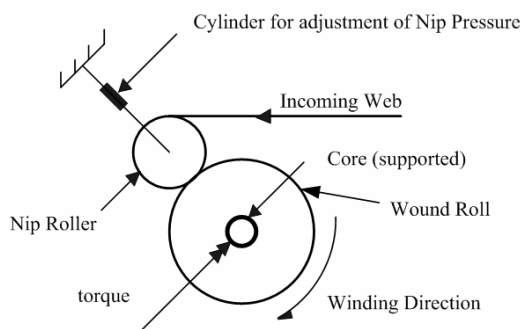


Fig. 6. A center winder with an impinging nip roller.

$$\sigma_w(r) = \sigma_0 \left[1 - \left(\frac{taper}{100} \right) \frac{(r-1)}{(r + \alpha \cdot (R-r-1))} \right] + \frac{\mu N(r)}{h} \tag{7}$$

2.3 Slippage between roller and moving web

A simple schematic of air film formed between moving web and roller by air entrainment is shown in Fig. 7. The entrained air causes a well known loss of traction force. In other words, desirable traction can be maintained when there is no air entrained between the web and roller. The air between web and roller lifts the web off when the operating speed is very high under a constant tension, because a traction force is reduced between web and roller. A low traction force between web and roller deteriorates the lateral stability of a moving web on a roller [13]. The slippage could be one of the major sources of the telescoping defect because the operating conditions of high speed and low tension are generally required in a winding process.

For the geometry and boundary conditions, the minimum thickness of air film was determined as shown in Eq. (8) [14-16].

$$h_o = 0.643R \left[\frac{6\eta(V_{web} + V_{roller})}{T} \right]^{2/3} \tag{8}$$

where η is the viscosity of air which varies with respect to the temperature. As webs pass over rollers subject to conditions of good traction, the velocity of web and roller is the same. Therefore, Eq. (8) can be rewritten as

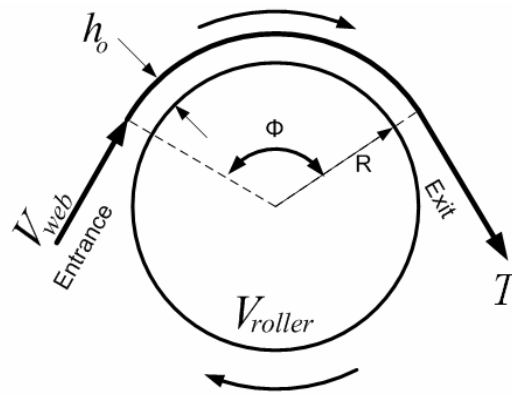


Fig. 7. Air films entrained between web and roll.

$$h_o = 0.643R \left[\frac{12\eta V}{T} \right]^{2/3} \quad (9)$$

Air film thickness (h_o) according to the operating tension variation from 0 to 100 N/m with constant velocity of 6 m/s, constant value of the viscosity ($\eta = 18.3 \times 10^{-6}$) at normal temperature is shown in Fig. 8. As the operating tension is increased, the air film thickness between web and roller becomes smaller. In other words, the possibility of slippage between roller and web can be large when the air film thickness is increased. It can be easily found that tension and velocity of a web are the principal and controllable operation parameters determining the air film thickness. Fig. 9 shows boundary conditions of slippage for a given range of tension and velocity. Although the thickness of air film in Eq. (9) is proportional to the two-thirds power of V/T , it looks like being almost linear in the small range of operating conditions as shown in Fig. 9.

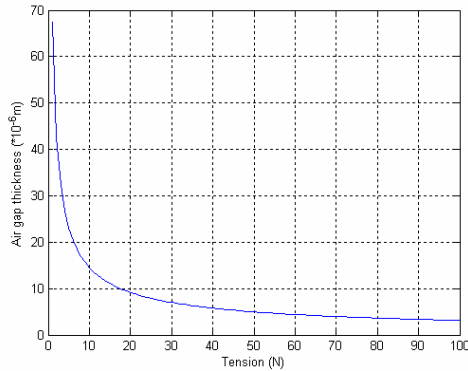


Fig. 8. Effect of web tension on air film thickness.

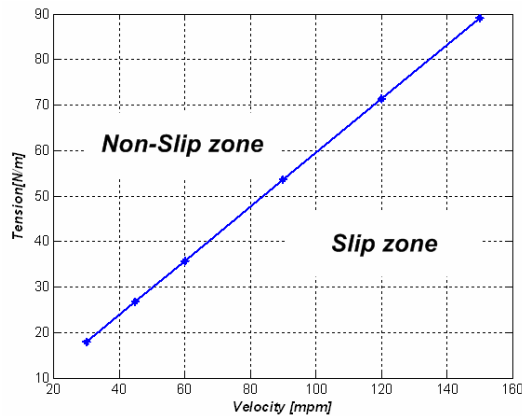


Fig. 9. Correlation between slippage and operating conditions.

The slippage is not in connection with the value of operating tension and speed but in relation to the ratio of operating speed and tension. Note that the winding tension should be decreased according to the build-up ratio under the condition of a constant velocity in a winding process. Therefore, air entrainment between layers in a wound roll can easily occur and be severe in a winding. These two typical operating conditions in a winding process lead air entrainment phenomenon to be a serious problem. Finally, the state of traction between layers in a wound roll can easily move from non-slip condition to slip condition, which increases the lateral instability of a web and makes the defect (telescoping) frequently happen.

2.4 Correlation between taper tension profile and telescoping

Telescoping in a wound roll can be assumed to be the result of lateral motion of a moving web during the winding process as discussed in the previous section. A mathematical model of the lateral motion was derived and analyzed by considering a web of elastic beam which curves in an arc or camber. Camber is the radius of curvature of a web under unforced condition lying on a flat surface. Assumed non-uniform stress distribution was applied on the cambered web as shown in Fig. 10; the induced moment is defined in Eq. (10) [10-12].

$$M = r \times F = \left(\frac{W}{6} \right) (T_{\max} - T_{\min}) = \frac{(T_{\max} - T_{\min})}{6} W \quad (10)$$

From the beam theory, curvature is defined as

$$\rho = \frac{EI}{M} \quad (11)$$

Substituting M of Eq. (11) into Eq. (10) leads to the curvature model of a cambered web as shown in Eq. (12).

$$\rho = \frac{6EI}{(T_{\max} - T_{\min})W} \quad (12)$$

In Fig. 11, lateral deflection of a web at a downstream roller is shown in Eq. (13) in which L , K mean length of span and stiffness coefficient, respectively [11].

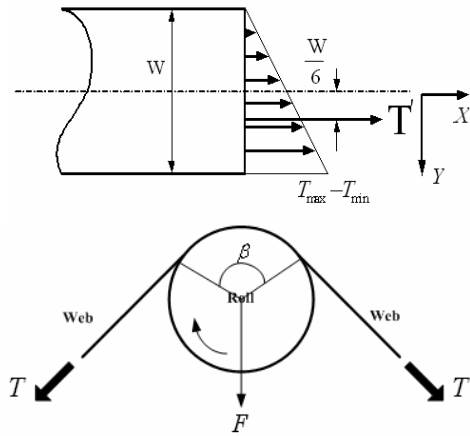


Fig. 10. Uneven tension distribution in CMD and wrap angle.

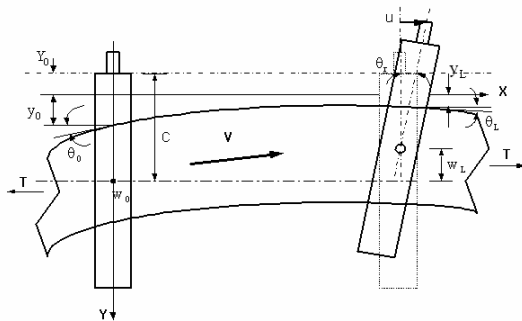


Fig. 11. Boundary condition in a span.

$$y_L = \frac{2 - 2 \cosh(KL) + \sinh(KL)KL}{\rho K^2 (\cosh(KL) - 1)} \quad (13)$$

The y_L in Eq. (13) is the lateral position of a moving web on a roller. It can be also considered as telescoping, because the downstream roller in Fig. 11 can be assumed to be a wound roll in a winding process.

Therefore, the mathematical model of telescoping can be derived in Eq. (14) by substituting Eq. (12) into Eq. (13).

$$y_{telescoping} = \frac{2 - 2 \cosh(KL) + \sinh(KL) \cdot KL}{\left[\frac{12EI}{(F_{max} - F_{min})W} \sin\left(\frac{\beta}{2}\right) \right] K^2 (\cosh(KL) - 1)} \quad (14)$$

where, F is force given by web tension and β is wrap angle. Non-uniform tension distribution shown in Fig. 10 can be generated from misalignment of rollers, slippage between roller and web, non-uniform

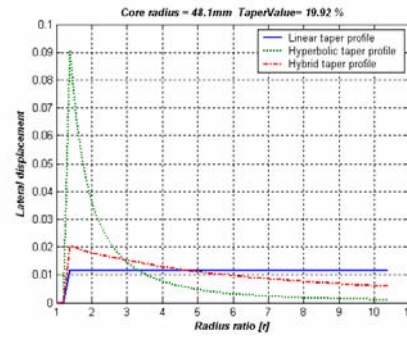


Fig. 12. Effect of taper tension profile on telescoping in a wound roll.

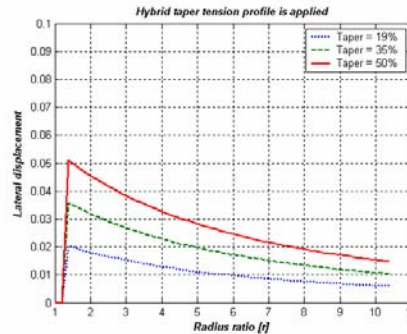


Fig. 13. Effect of taper value on telescoping in a wound roll.

nip force, etc. Additionally, in Eq. (14), a telescoping could be estimated by using a transverse winding tension ($F_{max} - F_{min}$) without additional edge position sensor.

A numerical simulation study was carried out to analyze the relationships between taper tension type and telescoping phenomenon under the condition of uneven tension distribution in cross machine direction. From Fig. 12, it was found that taper tension type can affect the magnitude of telescoping under the same taper value (19.92 %) because they have quite different tension variation according to the winding radius. It was also found that the telescoping problem could be serious at the beginning of rewinding process ($r < 2$). The telescoping defect for linear taper tension is very small in the initial stage of winding, which means that a linear taper tension profile is more effective to minimize telescoping. However, the telescoping for hyperbolic taper tension profile is low in the latter half of winding because the decrement of taper tension is smaller than that of linear taper tension profile. In general, taper value (*taper*) could be increased to minimize an excessive radial stress in a wound roll. However, Fig. 13 shows that the telescoping became

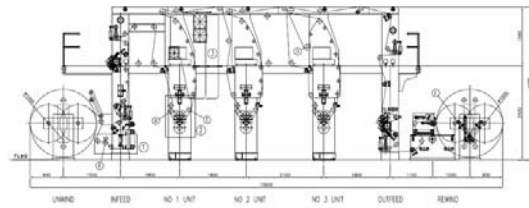


Fig. 14. Commercial roll to roll printing systems.

large in the wound roll when taper value was increased. Note that the value of telescoping is greatly influenced not by the magnitude of taper tension but by the decrement of taper tension.

3. Experimental verification

Commercial roll to roll printing systems, which were used for the experiment, are composed of unwinding, in-feeding, printing, out-feeding, and winding section as shown in Fig. 14. This experimental apparatus has the capacity of maximum speed 500 MPM and operating tension 200 N/m. A taper tension control is applied to winding system of roll to roll printing systems.

3.1 Experimental set up

The test machine consisted of unwinding, infeeding, printing, outfeeding, winding, and instruments including load cells, edge position sensors and encoder for measurement. The winding process was composed of a core, winding shaft, a lay on roll, a winding motor, a motor driver as shown in Fig. 15 and Fig. 16. A dancer system for taper tension control was installed as shown in Fig. 17. The lay-on roll for preventing air entrainment was covered with rubber. The dancer system for taper tension control was installed in the

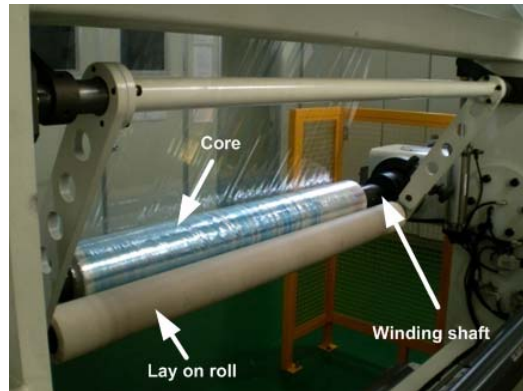


Fig. 15. Winding process.



Fig. 16. Winding drive systems.

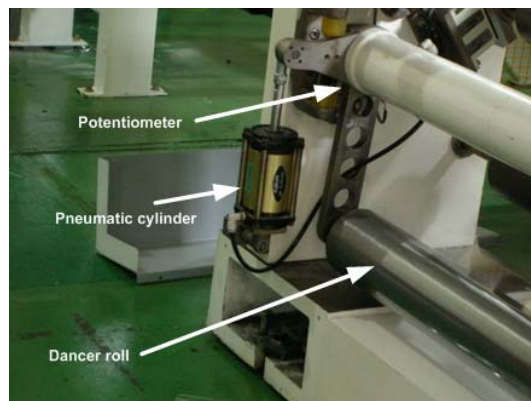


Fig. 17. Dancer system for taper tension control.



Fig. 18. Edge position sensor (IR) and amplifier.



Fig. 19. Load cell and amplifier.



Fig. 20. Encoder for measurement speed of idle roller.

outfeeding section and had a pneumatic system, dancer roll, and rotary potentiometer as shown in Fig. 17.

An edge position sensor (Fife, Model No. SE-23) including amplifier was installed in the winding zone to measure the lateral displacement of a moving web as shown in Fig. 18. Load cell (Mitsubishi, Model No. LX-TD-909) with amplifier (Mitsubishi, LM-PC) was installed in the idle roll to measure the winding tension of both edges of a moving web as shown in Fig. 19. To measure the relative velocity between tangential speed of idle roll and moving web, an incremental encoder (Autonics, ENC) with the resolution (500 pulses per a revolution) was used as shown in Fig. 20. Digital data acquisition software (LabVIEW 8.2) was used for collecting and storing the data as shown in Fig. 21. The output signal of load

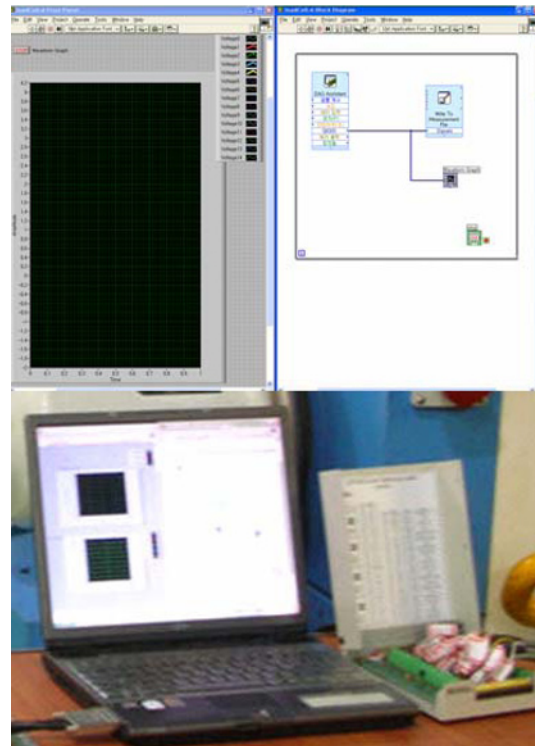


Fig. 21. Data acquisition systems.



Fig. 22. FSR (Force Sensing Resistor) sensor.

cell was connected to the analog input channel of data acquisition board (National Instruments, Model No. SCC-68), which was connected to the A/D converter (National Instruments, Model No. DAQ card-6062E). The data acquisition system was programmed to sample 5000 data points, and then their mean value was recorded. The nipping forces of lay-on roll were measured by FSR (Flexi Force, Model No. A101-100LB) as shown in Fig. 22.

3.2 Taper tension control systems

The taper tension control system was equipped for experimental study to verify the performance of the

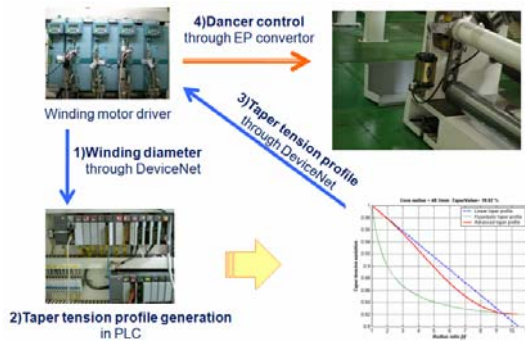


Fig. 23. Schematic of taper tension control system in roll to roll printing systems.

proposed taper tension profile as shown in Fig. 23. The current radius of winding roll is calculated by motor driver (SSD, Model No. 890), which is transmitted to the main controller (Allen Bradley, Model No. SLC 500) by DeviceNet protocol (Allen Bradley, Model No. 1747-SDN). The taper tension calculation logic was programmed in the main controller, which automatically generates a taper tension profile at every sampling period by using input data (winding radius) of the current state of the winding process. The updated reference taper tension is transmitted to the motor driver which controls the dancer position by adjusting rotational speed of winding roll to follow the reference taper tension.

3.3 Experiments on NIT

As discussed in section 2.2, a nip roll (lay-on roll) is installed to help exude wound-in air from the wound roll. A compressive force by the lay-on roll generates an additional web tension (NIT). The nip force is measured at seven different locations in the cross machine direction as shown in Fig. 24. The effect of nip force on tension is very small for a given nip force, even though the transverse distribution of NIT is uneven as shown in Fig. 25. However, this non-uniform transverse nip force could cause undesirable effects such as excessive lateral displacement of web. The dimensionless average value of NIT from the measured nip force is 0.07.

3.4 Experiments on telescoping

In section 2.4, the telescoping model was proposed in Eq. (13). The telescoping could be greatly influenced by the taper tension type and taper value under the slip condition as shown in Fig. 26(b). The first



Fig. 24. Measurement of NIT by using FSR.

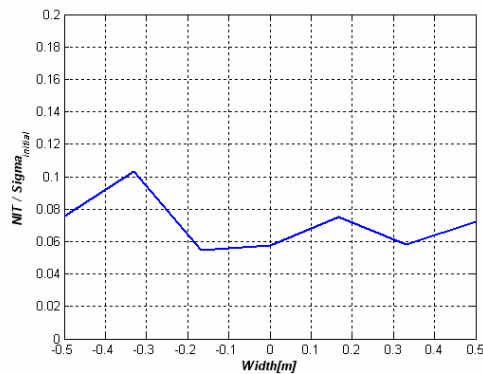
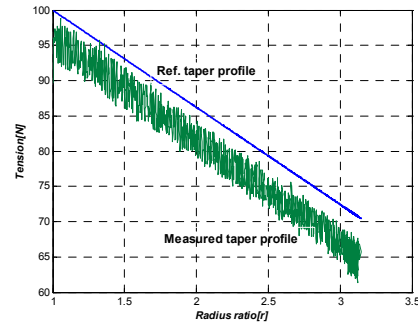


Fig. 25. Transverse nip induced tension distribution by lay-on roll.

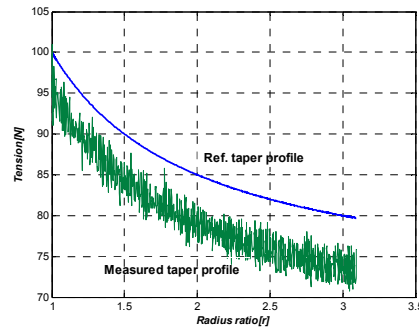
stage of experiments was focused on the validation of the telescoping model. At a certain test condition, the lateral displacement (telescoping) was measured by using the edge position sensor, and the taper tension variation was measured by the load cell at every experimental conditions. The values of the experiment parameters are tabulated in Table 1. Fig. 26 shows the web tension and velocity of both idle roll and web in winding process. From this experimental result, it is observed that the operating condition of 400 MPM and 142 N is one of the slip conditions which was introduced in section 2.3, saying that the operating conditions of high speed and low tension make it easy to cause the lateral instability of a moving web. The experimental studies on the telescoping were carried out for two types of taper tension in this slip condition. The one is a linear taper tension profile as shown in Fig. 27(a), and the other is a hyperbolic taper tension profile as shown in Fig. 27(b). Note again that the linear taper tension profile was recommended for reducing the telescoping because the variation of

Table 1. Telescoping test conditions.

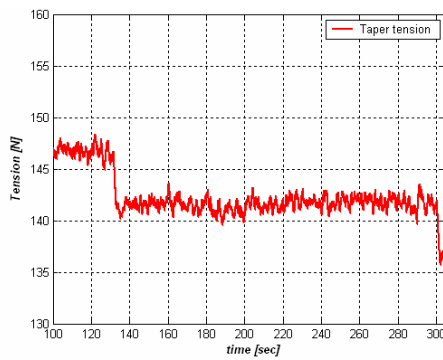
Parameter	Value
Substrate	PET
Web thickness	0.00014 m
Web width	1.01 m
Young's modulus (E)	$1180 \frac{N}{m^2}$
Operating speed	400 MPM
Operating tension	100 N
Maximum build up ratio of wound roll	3.1
Taper tension profile	Linear and hyperbolic type
Taper value	20 %
Poisson's ratio of web	0.3
Length of span in winding system (L)	6 m
Moment of inertia (I)	$1.0 \times 10^{-6} m^4$
Stiffness coefficient ($K(r)$)	$\sqrt{\frac{T(r)}{EI}} m^{-1}$
RMS roughness of the roller and web	$4.4 \times 10^{-6} m$



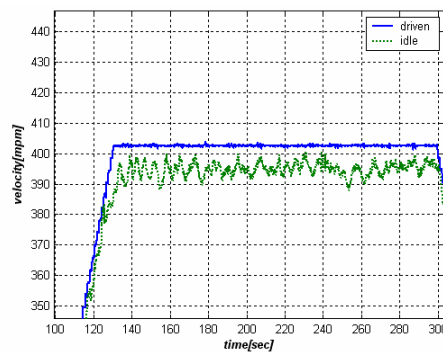
(a) Linear taper tension



(b) Hyperbolic taper tension



(a) Tension variations



(b) Velocity variations (web and idle roll)

Fig. 26. Correlation between slip and operating conditions.

Fig. 27. Taper tension variations in a winding system.

taper tension is smaller than the hyperbolic taper profile in the initial stage of a winding. Each Figure shows that the realized web tension correctly follows the reference taper tension profile within 5% variation from the desired tension reference. Therefore, the dancer is acceptable as a tension control system. However, there is an offset in magnitude between reference and actual profiles that is from the calibration error of load cell and amplifier.

A comparison between the estimated telescoping and measured telescoping at 400 MPM is shown in Fig. 28 and Fig. 29 for two types of taper tension profile. The measured telescoping is obtained by an edge position sensor, and the estimated telescoping is calculated using the proposed model. It is found that the mathematical model describing the telescoping phenomenon can properly estimate the tendency of telescoping in a winding process as shown in Fig. 28 and Fig. 29. However, the magnitude of measurement results shown in Fig. 28(a) and Fig. 29(a) is bigger than the results of estimation shown in Fig. 28(b) and Fig. 29(b). It is suspected that the difference is due to inaccuracy of load cell measurement and non-uniformity of nip pressure of lay-on roller. Additionally, much smoother surface roughness between layers

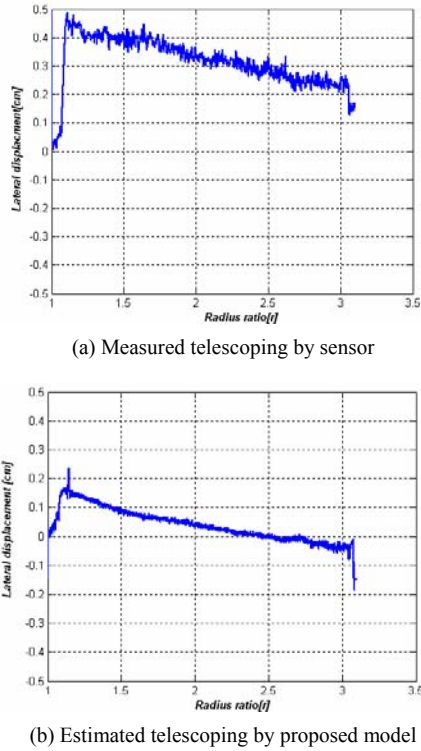


Fig. 28. Telescoping (linear taper tension).

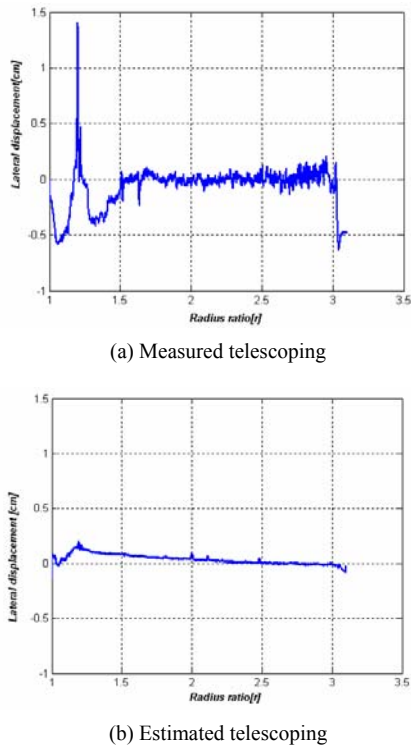
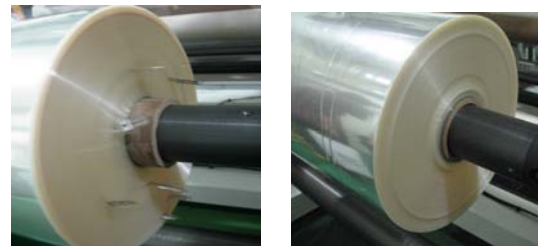


Fig. 29. Telescoping (hyperbolic taper tension).

in a wound roll than that between web and roller contributes to this result, because the layers in a wound roll are more slip than expected slip condition based on smooth web and rough roller surface. It is observed that the lateral displacement (telescoping) was raised up and changed abruptly in the case of hyperbolic taper tension profile by comparing Fig. 28 and Fig. 29. As discussed in section 2.3, the telescoping defect due to slippage between web and roller can be greater when the operating tension is reduced rapidly under the same speed in hyperbolic taper tension profile. It is found that the theoretical estimations can properly predict the trend of telescoping, although there are some differences between measured and estimated telescoping value. It is consistently shown that the telescoping became more serious when the hyperbolic taper tension profile was applied in a winding process. As found in the theoretical study, the telescoping value for a linear taper tension profile is very small in the initial stage of winding, but the magnitude of telescoping for a hyperbolic taper tension profile becomes smaller in the latter half of winding. It is the reason that the telescoping is affected by the decrement of tension. Fig. 30 represents the pictures of a wound roll that was fabricated with different taper tension profiles. More serious telescoping defect was observed in the initial stage of a wound roll when the hyperbolic taper tension profile was applied.

Therefore, the proposed model can be used in estimating the telescoping without lateral position sensor. This comparison shows the feasibility of the mathematical model to predict the telescoping defect in a winding system even though there is a difference of the telescoping value. From experimental results, it is found that a linear taper tension profile could be very effective to minimize telescoping defects in a wound roll.



(a) With linear taper tension (b) With hyperbolic taper tension

Fig. 30. Wound roll.

4. Conclusions

The effect of taper tension profile during the winding process on telescoping was analyzed, which affects the wound roll quality and productivity of final product in roll to roll printing systems.

The following conclusions can be drawn from this study:

- (1) A mathematical telescoping model is developed and verified experimentally by using commercial roll to roll printing systems.
- (2) It is analyzed and verified experimentally that slippage is induced frequently in a winding process because tension is decreased for a constant operating speed with respect to build up ratio.
- (3) A correlation between slippage and lateral behavior of a moving web in a winding process is analyzed and verified by experimental studies for given operating conditions.
- (4) Through the correlation between taper tension profile and telescoping, it is confirmed that a linear taper tension profile is very effective for minimizing telescoping defect in the initial stage of winding.

Acknowledgment

This work was supported by the Seoul R&BD Program (No.10848), Korea and the Korea Foundation for International Cooperation of Science & Technology (KICOS) through a grant provided by the Korean Ministry of Education, Science & Technology (MEST) in K20701040600-09A0404-05410.

References

- [1] S. J. Burns, Richard, R. Meehan and J. C. Lambropoulos, Strain-based Formulas for Stresses in Profiled Center-Wound Rolls, *Tappi journal*, 82 (1999) 159-167.
- [2] J. K. Good, J. D. Pfeiffer and R. M. Giachetto, Losses in Wound-On-Tension in the Center Winding of Wound Rolls, *Proceedings of the Web Handling Symposium, ASME Applied Mechanics Division*, 149 (1992) 1-12.
- [3] C. W. Lee, J. W. Lee, K. H. Shin and S. O. Kwon, A taper tension profile maker in a converting machine, *Journal of Mechanical Science and Technology*, 22 (2008) 77-84.
- [4] C. W. Lee, J. W. Lee and K. H. Shin, A study on the optimal taper tension control in a roll to roll machine, *The International Conference on Computational Science and Its Applications*, Part2 (2007) 919-930.
- [5] D. R. Roisum, Runnability of Paper Par2 : Trouble-shooting Web Breaks, *Tappi Journal*, 73 (1990) 101-106.
- [6] D. R. Roisum, Winder Vibration Can Reduce Operating Efficiency, *Tappi Journal*, 71 (1988) 87-96.
- [7] Z. Hakiel, Nonlinear model for wound roll stresses, *Tappi journal*, 70 (1987) 113-117.
- [8] C. Heinz and Altmann, Formulas for Computing the Stresses in Center-Wound Rolls, *Tappi journal*, 51 (1968) 176-179.
- [9] H. P. Yagoda, Resolution of a Core Problem in Wound Rolls, *Journal of Applied Mechanics*, 47 (1980) 847-854.
- [10] J. Shelton, Lateral Dynamics of a Moving Web, *Ph. D. dissertation Oklahoma state Univ. Stillwater*, (1968).
- [11] J. Shelton and K. N. Reid, Lateral Dynamics of a Real Moving Web, *ASME Journal Dynamics, Syst., Measurement, Control*, 93 (1971) 180-186.
- [12] J. Shelton, The Effect of Camber on Handling, *Proceedings of the International Conference on Web Handling*, Oklahoma state Univ. Stillwater, (1997) 248-263.
- [13] K. H. Shin and S. O. Kwon, The Effect of Tension on the Lateral Dynamics and Control of a Moving Web, *IEEE Trans. on Industry Applications*, 43 (2007) 403-412.
- [14] K. S. Ducotey and J. K. Good, The Effect of Web Permeability and Side Leakage on the Air Film Height Between a Roller and Web, *ASME Journal of Tribology*, 120 (1998) 559-565.
- [15] K. S. Ducotey and J. K. Good, Predicting Traction in Web Handling, *ASME Journal of Tribology*, 121 (1999) 618-624.
- [16] K. S. Ducotey and J. K. Good, A Numerical Algorithm for Determining the Traction Between a Web and a Circumferentially Grooved Roller, *ASME Journal of Tribology*, 122 (2000) 578-584.



Changwoo Lee (S'01–M'03) received a B.S. degree in Mechanical Engineering from Konkuk University in 2001. He received his M.S. and Ph.D. degrees from Konkuk university in 2003 and 2008, respectively.

He is currently a research professor at the Flexible Display Roll to Roll Research Center at Konkuk University in Seoul, Korea, where he is working on the development of R2R multi-layer printing systems for printed electronics. His research interests are in the area of fault tolerant control, R2R e-Printing line design, non-contact transporting process, and tension-register control. He is the holder of several patents related to R2R e-Printing system.



Keehyun Shin (S'81–M'87) received the B.S. degree from Seoul National University, Seoul, Korea, and the M.S. and Ph.D. degrees in mechanical engineering from Oklahoma State University (OSU), Stillwater. Since 1992, he has been

a Professor with the Department of Mechanical Engineering, Konkuk University, Seoul, Korea and director of Flexible Display Roll to Roll Research Center. For more than 18 years, he has covered several research topics in the area of web handling, including tension control, lateral dynamics, diagnosis of defect rolls/rollers, and fault-tolerant real-time He is the author of *Tension Control* (Atlanta, GA: TAPPI Press, 2000) and is the holder of several patents related to R2R e-Printing systems.